



PCCP

**A General Binary Isotherm Model for Amines Interacting
with CO₂ and H₂O**

Journal:	<i>Physical Chemistry Chemical Physics</i>
Manuscript ID	CP-ART-02-2023-000624.R1
Article Type:	Paper
Date Submitted by the Author:	13-Apr-2023
Complete List of Authors:	Kaneko, Yuta; Arizona State University, School of Sustainable Engineering and the Built Environment Lackner, Klaus; Arizona State University School of Sustainable Engineering and the Built Environment

SCHOLARONE™
Manuscripts

Cite this: DOI: 00.0000/xxxxxxxxxx

A General Binary Isotherm Model for Amines Interacting with CO₂ and H₂O

Yuta Kaneko^a and Klaus S. Lackner^a

Received Date

Accepted Date

DOI: 00.0000/xxxxxxxxxx

CO₂ capture by primary or secondary amines has been of great research interests for a century because of its industrial importance. Interest has grown even more, because of the need to eliminate the CO₂ emissions that drive global warming. Experimental evidence shows that CO₂ sorption in primary or secondary amines is accompanied by co-absorption of H₂O. A quantitative analysis of such CO₂-H₂O co-absorption behavior is important for practical process design and theoretical understanding. Even though there is almost an experimental consensus that water enhances CO₂ uptake capacity, an analytic model to explain this phenomenon is not well established. Instead, some empirical models such as the Toth model are used to describe the isotherm without accounting for the presence of water. Recently, we have demonstrated that the isotherm equation of CO₂ sorption into strong-base anion exchange materials with quaternary ammonium can be derived from that of strong-base aqueous alkaline solutions by correcting for the drastic change in water activity and by including an appropriate parameterization of the water activity terms. In this paper, we generalize this model from quaternary ammonium to primary, secondary and tertiary amines either in solutions or as functional groups in polymer resins. For primary, secondary and tertiary amines, the isotherm equation can be derived by extending that of a weak-base aqueous alkaline solution such as aqueous ammonia. The model has been validated using experimental data of aqueous ammonia in literature. This general model even includes quaternary ammonium as a special limit. Hence, this general model offers a platform that can treat the isotherms of solid amines, aqueous amines and aqueous alkaline solutions in a unified way.

1 Introduction

CO₂ absorption into primary, secondary or tertiary amines have been investigated for a century because of their industrial importance and scientific curiosity. From an industrial point of view, the basic process of CO₂ scrubbing from flue gas by aqueous amines was patented as early as 1930^{1,2}. Shortly after, Gregory and Scharmann (1937) from Standard Oil Company of Louisiana and Standard Oil Development Company presented experimental pilot plant data on CO₂ scrubbing using primary, secondary and tertiary amines (monoethanolamine, diaminopropanol and triethanolamine, respectively) from hydrogenation process gas³. From a theoretical perspective, the basic mechanism of CO₂ absorption into primary, secondary and tertiary amines has been proposed by researchers such as Goodridge (1955)⁴, Danckwerts (1979)⁵ and Donaldson & Nguyen (1980)⁶.

Since the comprehensive investigations by these pioneers, many researchers have pointed out an interesting, experimentally observed feature of this sorption system: the CO₂ sorption in primary or secondary amines is accompanied by co-absorption of H₂O^{4,7}. Today, there is a general consensus among experimentalists that the presence of water enhances the CO₂ uptake capacity of these sorbents. However, an isotherm equation that explicitly includes the influence of water has not yet been derived from the governing equations. Instead, some empirical models such as the Toth model⁸ have been used for CO₂ sorption isotherms for amine-functionalized silica, cellulose, and commercially-available weakly basic anion exchange resin such as Lewatits® VP OC 1065 in prior research, all of which contain primary, secondary or tertiary amines^{9–12}. The Toth model is an empirical extension of the Langmuir isotherm, which improves the fit both at low and high pressure⁸. The impact of water on the CO₂ isotherm is only captured by fitting parameters that vary with the water vapor pressure over the sorbent.

On the other hand, a strong-base anion exchange material (AEM) with quaternary ammonium in a hydroxide-carbonate-

^a School of Sustainable Engineering & the Built Environment, Arizona State University, Tempe, AZ 85287, United States. E-mail: ykaneko1@asu.edu, Klaus.Lackner@asu.edu

† Electronic Supplementary Information (ESI) available. (TBD)

bicarbonate form can also bind CO_2 through chemical reaction with hydroxide ions. In the 2000's, it has been experimentally observed that the CO_2 affinity of a strong-base anion exchange resin is affected by humidity levels, which points to the presence of moisture-swing or moisture-controlled CO_2 sorption^{13–16}. In this system, CO_2 is sorbed when the sorbent is dry, and CO_2 is desorbed when the sorbent is wet^{17–19}. Interestingly, such negative correlation between water and CO_2 sorption in quaternary ammonium is opposite to co-absorption observed in primary amines or secondary amines. In a previous paper, we have demonstrated that the CO_2 isotherm equation of a strong-base AEM can be derived by extending the theory of strong-base aqueous alkaline solutions^{20,21}. The resulting isotherm equation explicitly includes the water concentration term and thus can quantitatively account for the influence of water. The model predicts that raising the humidity of the surrounding gas results in the deviation from the Langmuir isotherm, which has been validated using literature data. Analogously, we hypothesize here that the deviation of CO_2 sorption isotherms of primary, secondary and tertiary amines from the Langmuir isotherm could be explained analytically in terms of the governing equations instead of adopting empirical models such as the Toth model.

In this paper, we extend the concepts we applied to moisture-controlled strong based AEMs to AEMs functionalized by primary, secondary and tertiary amines. The model also describes aqueous solutions of these amines, as well as ammonia. Therefore, in the next section, we briefly reviews the chemistry of CO_2 —amine systems to clarify the difference of CO_2 capture mechanisms among primary amines, secondary amines, tertiary amines and quaternary ammonium. In the theory section in this paper, all of these cases are unified into a single general model. In the result section, we validate this model using the experimental data of aqueous ammonia in the literature.

2 Review of CO_2 capture mechanism

We begin by reviewing the mechanisms for CO_2 capture in different amine configurations. For primary and secondary amines, sorption can occur in a nearly water-free environment, but water will strongly influence the reaction pathways. For tertiary amines, all possible reactions require the presence of water. Quaternary ammonium sorption also involves water.

2.1 CO_2 capture by Primary, Secondary and Tertiary Amines

The chemical reaction of CO_2 with primary amines (RNH_2) comprises two sequential elementary reactions^{5,16}. The first step forms the carbamic acids (RNHCOOH) as:



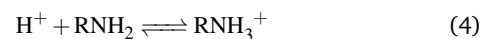
In an aqueous environment, the carbamic acid is almost completely dissociated to RNHCOO^- and H^+ ⁶ as:



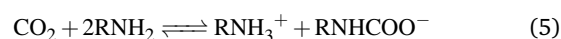
This proton is picked up by another primary amine to cause the second reaction that forms ammonium carbamate ion pairs ($\text{RNHCOO}^- + \text{RNH}_3^+$) as^{5,6}:



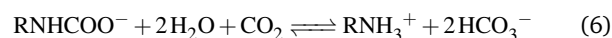
or,



Although this paper is focused on equilibrium considerations, not kinetics, it has been observed in literature that Eq.(1) is the rate-limiting step and Eq.(4) occurs instantly^{5,6}. The overall reaction is

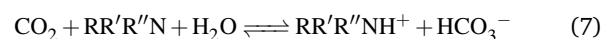


This overall equation indicates that the sorption of a CO_2 molecule requires two amine molecules: one to bind the CO_2 to the amine to form a carbamate ion, and the second to balance charge and bind the proton produced in the process by forming an ammonium ion. It is well-known that humidity enhances the CO_2 uptake of supported amine materials and raises their amine efficiency¹¹. In order to account for this mechanism, it has been pointed out that the following reaction additionally may occur to convert the carbamate ion to the bicarbonate in the presence of water^{4,7}:



This indicates that water enhances CO_2 sorption into primary amines. Under this condition, theoretical maximum sorption efficiency increases to one CO_2 molecule per nitrogen atom.

Essentially the same discussions as above apply to secondary amines by replacing RH with RR' in Eq.(1) through Eq.(6). However, in tertiary amines, CO_2 capture in anhydrous conditions does not occur because the tertiary amines do not have a proton to give⁴. Therefore, tertiary amines can capture CO_2 only by catalyzing the formation of bicarbonate according to the following chemical reaction^{6,22}:

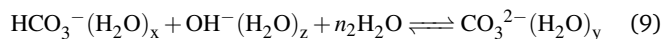
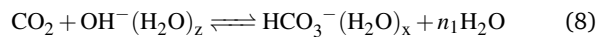


Namely, tertiary amines require water to capture CO_2 .

2.2 CO_2 capture by quaternary ammonium

The property and usage of quaternary ammonium are significantly different from those of primary, secondary and tertiary amines mainly because quaternary ammonium cannot release a proton and thus is always positively charged. Quaternary ammonium has been widely used in AEM membranes for electrodialysis or fuel cells. When the counter ion to the quaternary ammonium is a hydroxide ion, CO_2 reacts with the hydroxide and can be cap-

tured/released through the following chemical reactions^{18,19}:



where,

$$n_1 = -x + z \quad (10)$$

$$n_2 = -x + y - z - 1 \quad (11)$$

Note that x , y and z denote the number of hydration water molecules bound to each counter ion, HCO_3^- , CO_3^{2-} and OH^- , respectively. Keeping track of the total water is important in explaining the moisture effect on CO_2 sorption. At a partial pressure of 40Pa of CO_2 the relative humidity strongly affects the equilibrium loading of the strong-base ion exchange material. Finally, these chemical reactions indicate that the theoretical maximum amine efficiency is 0.5 when quaternary ammonium in a carbonate-bicarbonate form is used as moisture-controlled CO_2 sorbents.

2.3 Difference among quaternary ammonium and primary/secondary/tertiary amines

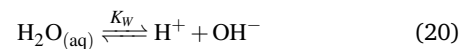
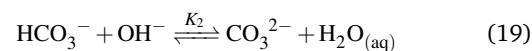
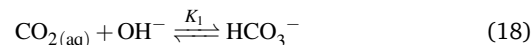
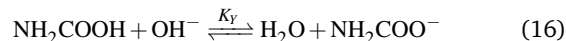
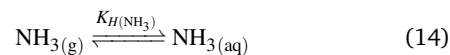
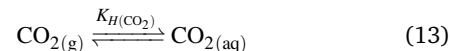
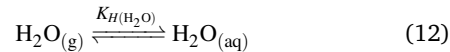
There are mainly two differences between quaternary ammonium and other amines. One is that primary and secondary amines not only catalyze hydration of CO_2 but also directly capture CO_2 to form carbamate while tertiary amines and quaternary ammonium capture CO_2 only by catalyzing hydration of CO_2 . Even though primary and secondary amines need no water for capture of CO_2 , their affinity to CO_2 is nevertheless profoundly affected by the presence of water. The other difference is that the base dissociation constant K_b needs to be introduced for weak-base such as primary, secondary and tertiary amines. Hence, we start with an isotherm theory of aqueous ammonia to construct a general model. This is similar to the approach taken for understanding strong-base anionic exchange resins in Kaneko & Lackner (2022a)²⁰.

3 Theory

In this paper, we keep track of all the chemical species and their transitions, but leave the relationship between water in the sorbent and the surrounding water vapor open, because it will vary from material to material. For example, the Flory-Huggins theory will apply to water absorption into anion exchange materials^{23,24}. Further work on specific sorbents is required to elucidate the water isotherm of a specific model.

3.1 Isotherm equation for aqueous ammonia

In aqueous ammonia, the following nine equations apply simultaneously²⁵:



where, apparent equilibrium coefficients and Henry's constants are defined as:

$$K_{H(\text{CO}_2)} \equiv \frac{[\text{CO}_2]}{P_{\text{CO}_2}} \quad (21)$$

$$K_{H(\text{NH}_3)} \equiv \frac{[\text{NH}_3]}{P_{\text{NH}_3}} \quad (22)$$

$$K_X \equiv \frac{[\text{NH}_2\text{COOH}]}{[\text{NH}_3][\text{CO}_2]} \quad (23)$$

$$K_Y \equiv \frac{[\text{NH}_2\text{COO}^-]}{[\text{NH}_2\text{COOH}][\text{OH}^-]} \quad (24)$$

$$K_b \equiv \frac{[\text{NH}_4^+][\text{OH}^-]}{[\text{NH}_3]} \quad (25)$$

$$K_1 \equiv \frac{[\text{HCO}_3^-]}{[\text{CO}_2][\text{OH}^-]} \quad (26)$$

$$K_2 \equiv \frac{[\text{CO}_3^{2-}]}{[\text{HCO}_3^-][\text{OH}^-]} \quad (27)$$

$$K_W \equiv [\text{H}^+][\text{OH}^-] \quad (28)$$

Note that i in brackets as in $[i]$ represents the concentration of the chemical species i . K_b denotes the base dissociation constant of ammonia in aqueous solutions. Later, we will generalize the isotherm model for aqueous ammonia to weak acids such as amino acids or amphoteric compounds such as primary amines. For these compounds, the values of the acid dissociation constant, K_a , is well investigated and available in literature rather than K_b . Therefore, it is convenient to translate K_b to K_a or $\text{p}K_a$ using the equation:

$$pK_a + pK_b = pK_w \quad (29)$$

According to the literature the values of these equilibrium coefficients at 25°C are given as²⁶⁻³² :

$$K_{H(\text{CO}_2)}^\circ = 3.3 \times 10^{-7} \quad [\text{mol L}^{-1} \text{ Pa}^{-1}] \quad (30)$$

$$K_{H(\text{NH}_3)}^\circ = 6.0 \times 10^{-4} \quad [\text{mol L}^{-1} \text{ Pa}^{-1}] \quad (31)$$

$$K_X^\circ = 7 \times 10^0 \quad [\text{mol}^{-1} \text{ L}] \quad (32)$$

$$K_Y^\circ = 1.7 \times 10^7 \quad [\text{mol}^{-1} \text{ L}] \quad (33)$$

$$K_b^\circ = 1.8 \times 10^{-5} \quad [\text{mol L}^{-1}] \quad (34)$$

$$(\text{or } pK_a^\circ = 9.3) \quad (35)$$

$$K_1^\circ = 4.4 \times 10^7 \quad [\text{mol}^{-1} \text{ L}] \quad (36)$$

$$K_2^\circ = 4.6 \times 10^3 \quad [\text{mol}^{-1} \text{ L}] \quad (37)$$

$$K_W^\circ = 1.0 \times 10^{-14} \quad [\text{mol}^2 \text{ L}^{-2}] \quad (38)$$

Note that the superscript ($^\circ$) represents the values for aqueous ammonia at 25°C in the limit of zero ionic strength. In addition to the above mass action laws, conservation laws apply as well. Specifically, charge neutrality must be preserved globally and locally. Charge neutrality can be described as follows:

$$[A_{\text{eff}}] + [\text{H}^+] = [\text{HCO}_3^-] + 2[\text{CO}_3^{2-}] + [\text{OH}^-] \quad (39)$$

where,

$$[A_{\text{eff}}] \equiv [\text{NH}_4^+] - [\text{NH}_2\text{COO}^-] + [A_{\text{res}}] \quad (40)$$

Note that $[A_{\text{eff}}]$ represents the effective alkalinity. In contrast to strong-base alkaline solutions such as potassium hydroxide solutions, alkalinity in aqueous ammonia is not constant but a function of pH which is set by the equilibria defined by Eq.(16), Eq.(17) and Eq.(20). $[A_{\text{res}}]$ denotes contributions originating from other charged species that do not appear in the chemical reactions but can be part of the solution, e.g., Na^+ , Cl^- or Br^- . $[A_{\text{res}}]$ is defined as the sum of all the residual positive ions weighted with their charge minus the sum of all the residual negative charges weighted with their charge.

We define the molar density of the total nitrogen as $[N]$, which is constant. According to mass conservation,

$$[N] = [\text{RNHCOOH}] + [\text{RNHCOO}^-] + [\text{NH}_3] + [\text{NH}_4^+] \quad (41)$$

Substituting Eq.(23), Eq.(24) and Eq.(25) into Eq.(41) yields:

$$[\text{NH}_4^+] = \frac{K_b [N]}{K_b + [\text{OH}^-] + [\text{OH}^-] K_X [\text{CO}_2] + K_X K_Y [\text{CO}_2] [\text{OH}^-]^2} \quad (42)$$

Substituting Eq.(23), Eq.(24), Eq.(26), Eq.(27) and Eq.(42)

into Eq.(39) yields an essential equation of this system:

$$[A_{\text{res}}] + \frac{[N](K_b - K_X K_Y [\text{CO}_2] [\text{OH}^-]^2)}{K_b + [\text{OH}^-] + [\text{CO}_2](K_X [\text{OH}^-] + K_X K_Y [\text{OH}^-]^2)} = [\text{CO}_2](K_1 [\text{OH}^-] + 2K_1 K_2 [\text{OH}^-]^2) + [\text{OH}^-] \quad (43)$$

Eq.(43) is a quadratic equation for $[\text{CO}_2]$ and thus $[\text{CO}_2]$ can be explicitly expressed as function of only one variable, $[\text{OH}^-]$:

$$[\text{CO}_2] = f([\text{OH}^-]) \equiv \frac{\beta}{2\alpha} \left(\sqrt{1 - \frac{4\alpha\gamma}{\beta^2}} - 1 \right) \quad (44)$$

where,

$$\begin{aligned} \alpha &= [\text{OH}^-]^4 2K_X K_Y K_1 K_2 \\ &+ [\text{OH}^-]^3 K_X K_1 (K_Y + 2K_2) \\ &+ [\text{OH}^-]^2 K_X K_1 \end{aligned} \quad (45)$$

$$\begin{aligned} \beta &= [\text{OH}^-]^3 (2K_1 K_2 + K_X K_Y) \\ &+ [\text{OH}^-]^2 (K_1 + 2K_b K_1 K_2 + K_X + K_X K_Y ([N] - [A_{\text{res}}])) \\ &+ [\text{OH}^-] (K_b K_1 - K_X [A_{\text{res}}]) \end{aligned} \quad (46)$$

$$\gamma = [\text{OH}^-]^2 + [\text{OH}^-] (K_b - [A_{\text{res}}]) - K_b ([N] + [A_{\text{res}}]) \quad (47)$$

The other root of Eq.(43) always takes a negative value and thus is not physical. In this section, we assume $[A_{\text{res}}] \sim 0$ for simplification. In this case, β and γ simplify to:

$$\begin{aligned} \beta &= [\text{OH}^-]^3 (2K_1 K_2 + K_X K_Y) \\ &+ [\text{OH}^-]^2 (K_1 + 2K_b K_1 K_2 + K_X + K_X K_Y [N]) \\ &+ [\text{OH}^-] K_b K_1 \end{aligned} \quad (48)$$

$$\gamma = [\text{OH}^-]^2 + K_b [\text{OH}^-] - K_b [N] \quad (49)$$

Eq.(45), Eq.(48) and Eq.(49) indicate that γ can mathematically take negative values while α and β are guaranteed to be positive. However, substituting $\gamma > 0$ into Eq.(44) yields $[\text{CO}_2] < 0$. Therefore, there is a physical upper bound for $[\text{OH}^-]$ (i.e., $[\text{OH}^-]_{\text{max}}$) so that γ is kept negative or zero, which is discussed later in more detail. $\frac{\beta}{2\alpha}$, $\sqrt{1 - \frac{4\alpha\gamma}{\beta^2}} - 1$, γ and $[\text{CO}_2]$ are plotted in Fig.(1), Fig.(2), Fig.(3) and Fig.(4), respectively. These figures confirm the mathematical and physical limits summarized in Table.(1).

Conversely, $[\text{OH}^-]$ can be implicitly expressed as function of only one variable, $[\text{CO}_2]$:

$$[\text{OH}^-] = f^{-1}([\text{CO}_2]) \quad (50)$$

Table 1 Summary of small or large $[\text{OH}^-]$ limits. δ_1 and δ_2 in this table are positive numbers defined as $\delta_1 \equiv \sqrt{1 + \frac{4K_X[N]}{K_b K_1}} - 1$ and $\delta_2 \equiv -\frac{2K_1 K_2 + K_X K_Y}{4K_X K_Y K_1 K_2} \left(\sqrt{1 - \frac{8K_X K_Y K_1 K_2}{(2K_1 K_2 + K_X K_Y)^2}} - 1 \right)$, respectively. DIC1 stands for Dissolved Inorganic Carbon as Ions, namely, CO_3^{2-} and HCO_3^- .

parameter or variable	limit of a small $[\text{OH}^-]$	physical limit of a large $[\text{OH}^-]$	unphysical limit of a large $[\text{OH}^-]$
$[\text{OH}^-]$	$[\text{OH}^-] \rightarrow 0$	$[\text{OH}^-] \rightarrow [\text{OH}^-]_{\max}$	$[\text{OH}^-] \rightarrow \infty$
$\frac{\beta}{2\alpha}$	$\frac{K_b}{2K_X[\text{OH}^-]} \rightarrow \infty$	$\frac{2K_1 K_2 + K_X K_Y}{4[\text{OH}^-]_{\max} K_X K_Y K_1 K_2} \rightarrow \text{finite}$	$\frac{2K_1 K_2 + K_X K_Y}{4[\text{OH}^-] K_X K_Y K_1 K_2} \rightarrow +0$
$\sqrt{1 - \frac{4\alpha\gamma}{\beta^2}} - 1$	$\delta_1 \rightarrow \text{finite}$	0	$\sqrt{1 - \frac{8K_X K_Y K_1 K_2}{(2K_1 K_2 + K_X K_Y)^2}} - 1 < 0$
$[\text{CO}_2]$	$\frac{K_b}{2K_X[\text{OH}^-]} \delta_1 \rightarrow \infty$	0	$-\frac{\delta_2}{[\text{OH}^-]} < 0$
$[\text{A}_{\text{eff}}]$	$\frac{K_b K_1}{2K_X} \delta_1 \rightarrow \text{finite}$	$[\text{OH}^-]_{\max} \rightarrow \text{finite}$	$\frac{K_X K_Y [N] \delta_2}{1 - K_X K_Y \delta_2} \rightarrow \text{finite}$
$[\text{NH}_4^+]$	$\frac{K_b K_1}{2K_X} \delta_1 \rightarrow \text{finite}$	$[\text{OH}^-]_{\max} \rightarrow \text{finite}$	$\frac{K_b [N]}{[\text{OH}^-] (1 - K_X K_Y \delta_2)} \rightarrow 0$
$[\text{NH}_2\text{COOH}]$	$\frac{K_b K_1}{4K_X} \delta_1^2 \rightarrow \text{finite}$	0	$-\frac{K_X [N] \delta_2}{[\text{OH}^-] (1 - K_X K_Y \delta_2)} \rightarrow 0$
$[\text{NH}_2\text{COO}^-]$	$\frac{K_b K_1 K_Y [\text{OH}^-]}{4K_X} \delta_1^2 \rightarrow 0$	0	$-\frac{K_X K_Y [N] \delta_2}{1 - K_X K_Y \delta_2} \rightarrow \text{finite}$
$[\text{NH}_3]$	$\frac{K_1 [\text{OH}^-]}{2K_X} \delta_1 \rightarrow 0$	$\frac{[\text{OH}^-]_{\max}^2}{K_b} \rightarrow \text{finite}$	$\frac{[N]}{1 - K_X K_Y \delta_2} \rightarrow \text{finite}$
$[\text{HCO}_3^-]$	$\frac{K_b K_1}{2K_X} \delta_1 \rightarrow \text{finite}$	0	$-K_1 \delta_2 < 0$
$[\text{CO}_3^{2-}]$	$\frac{K_b K_1 K_2 [\text{OH}^-]}{2K_X} \delta_1 \rightarrow 0$	0	$-K_1 K_2 [\text{OH}^-] \delta_2 \rightarrow -\infty < 0$
θ_{DOC}	$\frac{K_b K_1}{4K_X [N]} \delta_1^2 \rightarrow \text{finite}$	0	$-\frac{K_X K_Y \delta_2}{1 - K_X K_Y \delta_2} \rightarrow \text{finite}$
θ_{DIC1}	$\frac{K_b K_1}{2K_X [N]} \delta_1 \rightarrow \text{finite}$	0	$-\frac{K_1 K_2 [\text{OH}^-] \delta_2}{[N]} \rightarrow -\infty < 0$
$\theta_{\text{DOC}} + \theta_{\text{DIC1}}$	1	0	$-\frac{K_1 K_2 [\text{OH}^-] \delta_2}{[N]} \rightarrow -\infty < 0$
θ	$1 + \frac{[\text{CO}_2]}{[N]} \rightarrow 1 + \infty$	0	$-\frac{K_1 K_2 [\text{OH}^-] \delta_2}{[N]} \rightarrow -\infty < 0$

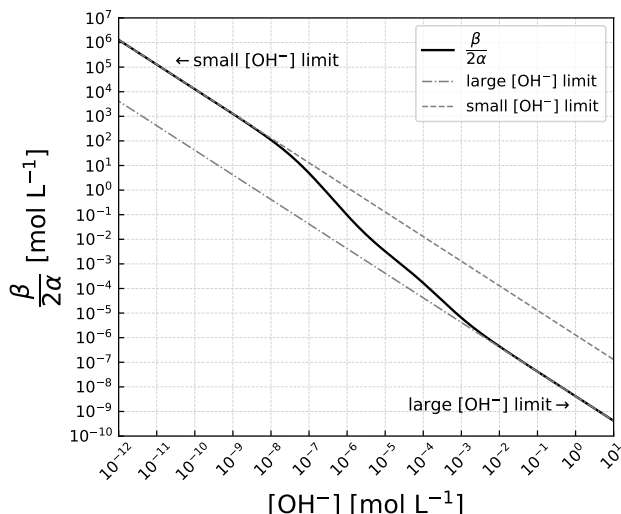


Fig. 1 $\frac{\beta}{2\alpha}$ as function of $[\text{OH}^-]$ for $[N] = 2 \text{ mol L}^{-1}$ and $T = 25^\circ\text{C}$.

By substituting Eq.(50) into Eq.(42), $[\text{NH}_4^+]$ can be implicitly expressed as function of only one variable, $[\text{CO}_2]$, as:

$$[\text{NH}_4^+] = \frac{K_b [N]}{K_b + f^{-1}([\text{CO}_2]) \{1 + K_X [\text{CO}_2] (1 + f^{-1}([\text{CO}_2]) K_Y)\}} \quad (51)$$

$$\equiv g([\text{CO}_2]) \quad (52)$$

Therefore, the effective alkalinity $[\text{A}_{\text{eff}}]$ can be expressed as:

$$[\text{A}_{\text{eff}}] = g([\text{CO}_2]) \times \left(1 - \frac{K_X K_Y}{K_b} [\text{CO}_2] \{f^{-1}([\text{CO}_2])\}^2 \right) \quad (53)$$

Fig.(5), Fig.(6) and Fig.(7) show plots of the effective alkalinity and concentration of each chemical species, assuming $[N] = 2 \text{ mol L}^{-1}$ and $T = 25^\circ\text{C}$.

The CO_2 loading status θ can be defined as:

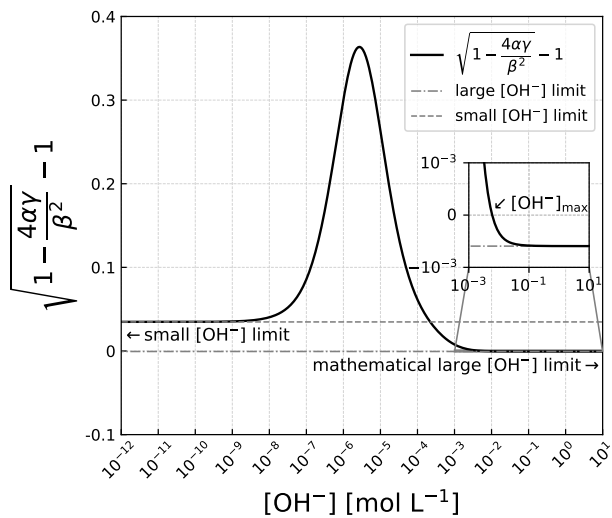


Fig. 2 $\sqrt{1 - \frac{4\alpha\gamma}{\beta^2}} - 1$ as function of $[\text{OH}^-]$ for $[\text{N}] = 2 \text{ mol L}^{-1}$ and $T = 25^\circ\text{C}$. Note that $\sqrt{1 - \frac{4\alpha\gamma}{\beta^2}} - 1$ takes negative values at $[\text{OH}^-] > [\text{OH}^-]_{\text{max}}$.

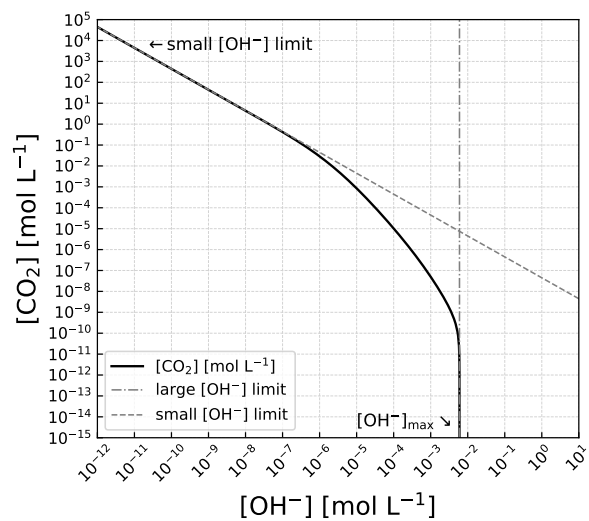


Fig. 4 $[\text{CO}_2]$ as function of $[\text{OH}^-]$ for $[\text{N}] = 2 \text{ mol L}^{-1}$ and $T = 25^\circ\text{C}$.

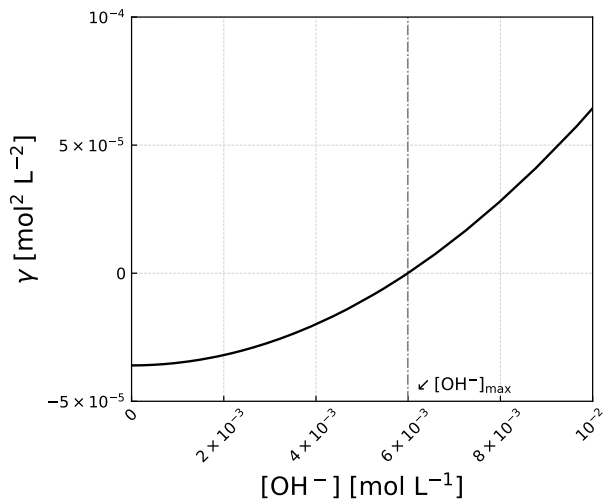


Fig. 3 γ as function of $[\text{OH}^-]$ for $[\text{N}] = 2 \text{ mol L}^{-1}$ and $T = 25^\circ\text{C}$.

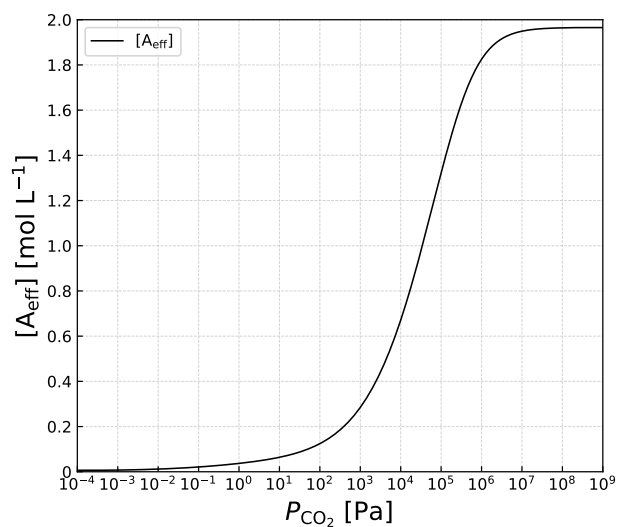


Fig. 5 The effective alkalinity $[\text{A}_{\text{eff}}]$ as function of P_{CO_2} for $[\text{N}] = 2 \text{ mol L}^{-1}$ and $T = 25^\circ\text{C}$.

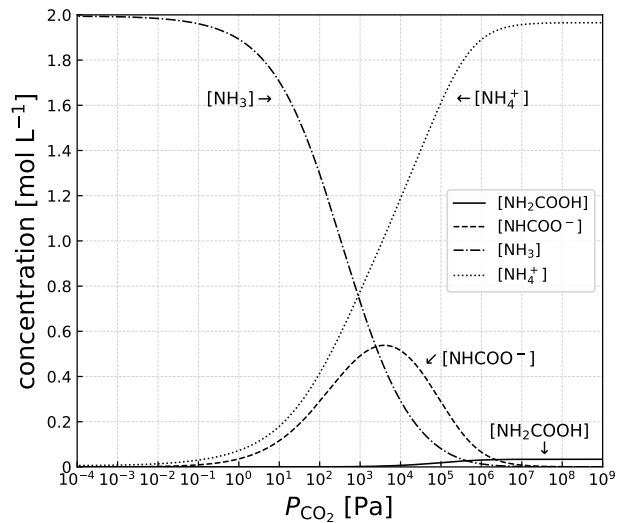


Fig. 6 Concentrations of DOC components as function of P_{CO_2} for $[\text{N}] = 2 \text{ mol L}^{-1}$ and $T = 25^\circ\text{C}$.

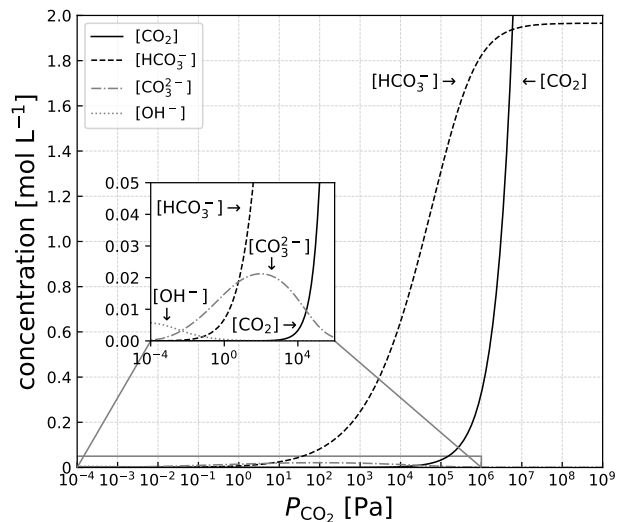


Fig. 7 Concentrations of DIC components and $[\text{OH}^-]$ as function of P_{CO_2} for $[\text{N}] = 2 \text{ mol L}^{-1}$ and $T = 25^\circ\text{C}$.

$$\theta \equiv \theta_{\text{DOC}} + \theta_{\text{DIC}} \quad (54)$$

where,

$$\theta_{\text{DOC}} \equiv \frac{[\text{DOC}]}{[\text{N}]} \quad (55)$$

$$\theta_{\text{DIC}} \equiv \frac{[\text{DIC}]}{[\text{N}]} \quad (56)$$

Note that DOC and DIC represent Dissolved Organic Carbon and Dissolved Inorganic Carbon, respectively, which are defined as:

$$[\text{DOC}] \equiv [\text{NH}_2\text{COOH}] + [\text{NH}_2\text{COO}^-] \quad (57)$$

$$[\text{DIC}] \equiv [\text{CO}_2] + [\text{HCO}_3^-] + [\text{CO}_3^{2-}] \quad (58)$$

Therefore,

$$\begin{aligned} \theta &= \frac{K_X}{K_b[\text{N}]} g([\text{CO}_2]) [\text{CO}_2] f^{-1}([\text{CO}_2]) \left(1 + K_Y f^{-1}([\text{CO}_2]) \right) \\ &+ \frac{[\text{CO}_2]}{[\text{N}]} \left(1 + K_1 f^{-1}([\text{CO}_2]) + K_1 K_2 \left\{ f^{-1}([\text{CO}_2]) \right\}^2 \right) \end{aligned} \quad (59)$$

This equation can be numerically plotted against P_{CO_2} or pH, as is shown in Fig.(8) and Fig.(9), assuming $[\text{N}] = 2 \text{ mol L}^{-1}$ and $T = 25^\circ\text{C}$.

3.1.1 Large $[\text{OH}^-]$ limit

Eq.(44) indicates that $[\text{CO}_2]$ becomes zero when $\gamma = 0$. In this case, $[\text{OH}^-]_{\text{max}}$ satisfies the following equation:

$$[\text{OH}^-]_{\text{max}}^2 + K_b[\text{OH}^-]_{\text{max}} - K_b[\text{N}] = 0 \quad (60)$$

or,

$$[\text{OH}^-]_{\text{max}} = \frac{K_b}{2} \left(\sqrt{1 + \frac{4[\text{N}]}{K_b}} - 1 \right) \quad (61)$$

If $[\text{OH}^-]$ exceeds $[\text{OH}^-]_{\text{max}}$, it results in $[\text{CO}_2] < 0$. Since $[\text{CO}_2]$ needs to be positive, $[\text{OH}^-]_{\text{max}}$ set the maximum pH of this system. Substituting $[\text{N}] = 2 \text{ mol L}^{-1}$ and Eq.(34) into Eq.(61) yields:

$$[\text{OH}^-]_{\text{max}} = 5.99 \times 10^{-3} [\text{mol L}^{-1}] \quad (62)$$

or,

$$\text{pH}_{\text{max}} = \text{pH}(\theta = 0) = 11.77 \quad (63)$$

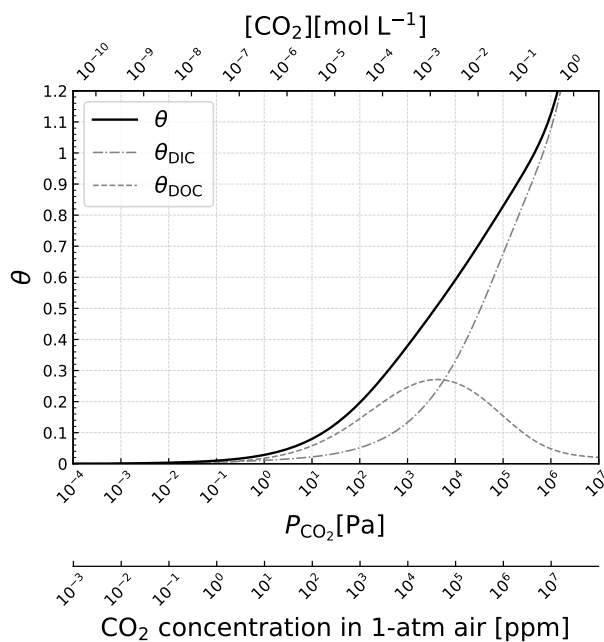


Fig. 8 θ and each component (θ_{DIC} and θ_{DOC}) as function of P_{CO_2} , $[\text{CO}_2]$ or CO_2 concentration in 1-atm air for $[\text{N}] = 2 \text{ mol L}^{-1}$ and $T = 25^\circ\text{C}$.

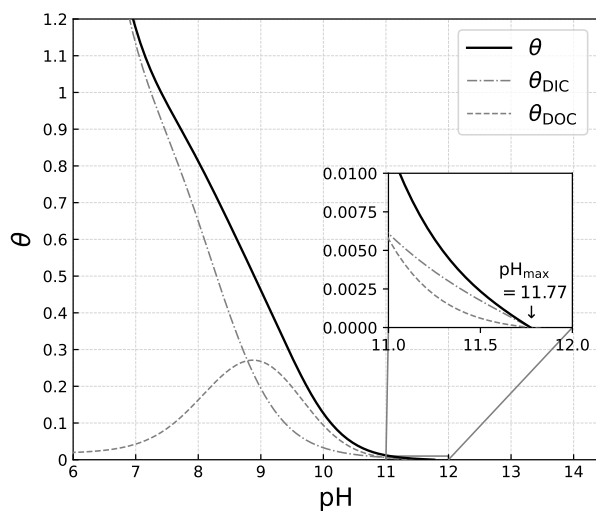


Fig. 9 θ and each component (θ_{DIC} and θ_{DOC}) as function of pH for $[\text{N}] = 2 \text{ mol L}^{-1}$ and $T = 25^\circ\text{C}$.

This value agrees with the pH of a 2 mol L^{-1} pure aqueous ammonia which does not include any DIC or DOC.

While this is the physically maximum limit of $[\text{OH}^-]$ which is corresponding to $[\text{CO}_2] = 0$, one can mathematically take the limit of $[\text{OH}^-] \rightarrow \infty$. Although this is an unphysical case because this mathematical limit results in negative values of $[\text{CO}_2]$, investigating this asymptotical behavior is useful to understand the global structure of the governing equation of this system, i.e., Eq.(44). Both unphysical limits (in other words, mathematical limits) and physical limits have been derived and summarized in Table.(1).

It is also notable that $[\text{A}_{\text{res}}]$ affects the value of $[\text{OH}^-]_{\text{max}}$ if $[\text{A}_{\text{res}}] \neq 0$. In this case, $[\text{OH}^-]_{\text{max}}$ can be expressed as:

$$[\text{OH}^-]_{\text{max}} = \frac{K_b - [\text{A}_{\text{res}}]}{2} \left(\sqrt{1 + \frac{4K_b([\text{N}] + [\text{A}_{\text{res}}])}{(K_b - [\text{A}_{\text{res}}])^2}} - 1 \right) \quad (64)$$

3.1.2 Small $[\text{OH}^-]$ limit

Fig.(5), Fig.(6) and Fig.(8) suggest that $[\text{A}_{\text{eff}}]$, $[\text{NH}_4^+]$, $[\text{NH}_2\text{COOH}]$ and θ_{DOC} converge to constant values in the limit of $[\text{CO}_2] \rightarrow \infty$ (in other words, in the limit of $[\text{OH}^-] \rightarrow 0$), respectively. The analytic expressions of these limits have been derived and summarized in Table.(1). For details, see the Supplementary Information.

3.1.3 Large K_b limit

When $K_b \gg [\text{OH}^-]$ is satisfied, Eq.(42) results in:

$$[\text{NH}_4^+] \sim [\text{N}] \quad (65)$$

Therefore,

$$[\text{RNH}_2] \sim 0 \quad (66)$$

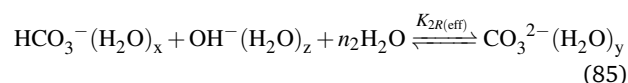
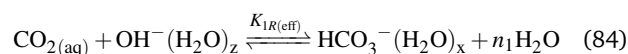
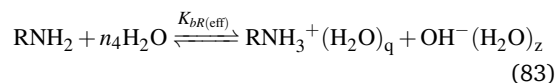
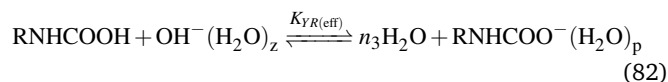
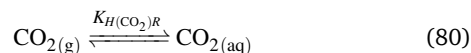
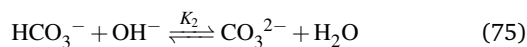
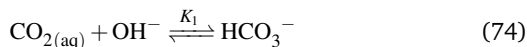
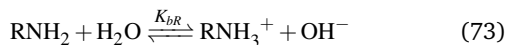
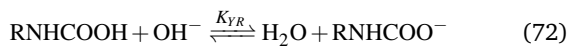
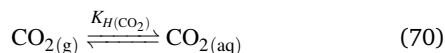
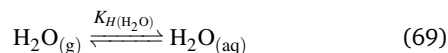
$$[\text{RNHCOOH}] \sim 0 \quad (67)$$

$$[\text{RNHCOO}^-] \sim 0 \quad (68)$$

In this limit, the model reduces to the isotherm model of alkaline aqueous solutions in a hydroxide-carbonate-bicarbonate system with a constant alkalinity of $[\text{N}]$, which is identical to the model derived in the previous paper²⁰.

3.2 Generalization to Aqueous Amine Solutions

In aqueous amine solutions, the equilibrium coefficients K_X , K_Y and K_b can differ from those in aqueous ammonia and will depend on specific materials used as a sorbent. Therefore, we rename these equilibrium coefficients depending on a specific amine as K_{XR} , K_{YR} and K_{bR} , respectively. In case of primary amines, the chemical reactions can be described as:



where, K_{XR} , K_{YR} and K_{bR} are defined as:

$$K_{XR} \equiv \frac{[\text{RNHCOOH}]}{[\text{NH}_3][\text{CO}_2]} \quad (76)$$

$$K_{YR} \equiv \frac{[\text{RNHCOO}^-]}{[\text{RNHCOOH}][\text{OH}^-]} \quad (77)$$

$$K_{bR} \equiv \frac{[\text{RNH}_3^+][\text{OH}^-]}{[\text{RNH}_2]} \quad (78)$$

In case of secondary amines, we need to replace RH by RR'. Therefore, essentially the same key equation (Eq.(44)) apply to aqueous primary and secondary amine solutions just by replacing K_X , K_Y and K_b with K_{XR} , K_{YR} and K_{bR} , respectively.

For tertiary amines, Eq.(71) and Eq.(72) do not apply. Therefore, we can obtain the model for tertiary amines by substituting $K_{XR} = 0$ and $K_{YR} = 0$. The resulting key equation for tertiary amines corresponding to Eq.(44) for primary and secondary amines can be expressed as:

$$[\text{CO}_2] = \frac{-[\text{OH}^-]^2 + [\text{OH}^-]([\text{A}_{\text{res}}] - K_{bR}) + K_{bR}([\text{A}_{\text{res}}] + [\text{N}])}{K_1[\text{OH}^-](1 + 2K_2[\text{OH}^-])(K_{bR} + [\text{OH}^-])} \quad (79)$$

3.3 Generalization to Amine Solids

The main difference between aqueous amine solutions and amine solids is that water concentration in amine solids is not large enough to be regarded as constant. Also, hydration water around ions need to be taken into consideration, as follows:

p , q , x , y and z represent hydration numbers of RNHCOO^- , RNH_3^+ , HCO_3^- , CO_3^{2-} and OH^- , respectively. The stoichiometric coefficients n_1 , n_2 , n_3 and n_4 can be expressed as:

$$n_1 = -x + z \quad (86)$$

$$n_2 = -x + y - z - 1 \quad (87)$$

$$n_3 = -p + z - 1 \quad (88)$$

$$n_4 = q + z + 1 \quad (89)$$

The equilibrium coefficients and Henry's constant are defined as:

$$K_{H(\text{CO}_2)R} \equiv \frac{[\text{CO}_2]}{P_{\text{CO}_2}} \quad (90)$$

$$K_{XR} \equiv \frac{[\text{RNHCOOH}]}{[\text{NH}_3][\text{CO}_2]} \quad (91)$$

$$K_{YR} \equiv \frac{[\text{RNHCOO}^- (\text{H}_2\text{O})_p][\text{H}_2\text{O}]^{n_3}}{[\text{RNHCOOH}][\text{OH}^- (\text{H}_2\text{O})_z]} \quad (92)$$

$$K_{bR} \equiv \frac{[\text{RNH}_3^+ (\text{H}_2\text{O})_q][\text{OH}^- (\text{H}_2\text{O})_z]}{[\text{RNH}_2][\text{H}_2\text{O}]^{n_4}} \quad (93)$$

$$K_{1R} \equiv \frac{[\text{HCO}_3^- (\text{H}_2\text{O})_x][\text{H}_2\text{O}]^{n_1}}{[\text{CO}_2][\text{OH}^- (\text{H}_2\text{O})_z]} \quad (94)$$

$$K_{2R} \equiv \frac{[\text{CO}_3^{2-} (\text{H}_2\text{O})_y]}{[\text{HCO}_3^- (\text{H}_2\text{O})_x][\text{OH}^- (\text{H}_2\text{O})_z][\text{H}_2\text{O}]^{n_2}} \quad (95)$$

Therefore, the same functional forms for aqueous amine solutions apply to solid amines by replacing K_{YR} , K_{bR} , K_1 and K_2 with $K_{YR(\text{eff})}$ ($\equiv K_{YR}[\text{H}_2\text{O}]^{-n_3}$), $K_{bR(\text{eff})}$ ($\equiv K_{bR}[\text{H}_2\text{O}]^{n_4}$), $K_{1R(\text{eff})}$ ($\equiv K_{1R}[\text{H}_2\text{O}]^{-n_1}$) and $K_{2R(\text{eff})}$ ($\equiv K_{2R}[\text{H}_2\text{O}]^{n_2}$), respectively. In the same way for moisture-controlled CO_2 sorption in quaternary ammonium discussed in the previous paper²⁰, the stoichiometric co-

efficients, n_1 , n_2 , n_3 and n_4 determine whether CO_2 affinity is enhanced or hindered due to the changes in the concentration of water inside the sorbent.

4 Result: Validation of the framework of the model using the literature data of aqueous ammonia

In the previous section, we generalized the isotherm model of aqueous ammonia to amines, which is represented by the key equation, Eq.(44). In this section, we calculate the CO_2 isotherms of aqueous ammonia and partial pressure of gaseous ammonia by substituting the specific values of the equilibrium coefficients from the literature into this key equation. The resulting CO_2 isotherms and P_{NH_3} of aqueous ammonia are compared to the experimental isotherm data from Pexton and Badger (1938)³³. Since this experimental data set was not obtained at 25 °C which is typically used as a modern standard, we calculate our model at 20°C and 40°C so that we can compare the model to the experimental data. Note that the isotherm data from Pexton and Badger (1938) has also been used in other research^{34–36} to compare to the two thermodynamic models for electrolyte solutions: the extended universal quasichemical (UNIQUAC) model^{36,37} and the Electrolyte Non Random Two Liquid (e-NRTL) model^{38,39}.

The values of K_H , K_1 , K_2 and K_W for the temperature ranging from 0°C to 40°C are given as function of the temperature T in the literature^{26–28}. Substituting $T = 20^\circ\text{C}$ or $T = 40^\circ\text{C}$ into these equations yields:

$$K_{H(\text{CO}_2)}(T = 20^\circ\text{C}) = 3.8 \times 10^{-7} \quad [\text{mol L}^{-1} \text{ Pa}^{-1}] \quad (96)$$

$$K_1(T = 20^\circ\text{C}) = 6.1 \times 10^7 \quad [\text{mol}^{-1} \text{ L}] \quad (97)$$

$$K_2(T = 20^\circ\text{C}) = 6.1 \times 10^3 \quad [\text{mol}^{-1} \text{ L}] \quad (98)$$

$$K_W(T = 20^\circ\text{C}) = 6.8 \times 10^{-15} \quad [\text{mol}^2 \text{ L}^{-2}] \quad (99)$$

$$K_{H(\text{CO}_2)}(T = 40^\circ\text{C}) = 2.3 \times 10^{-7} \quad [\text{mol L}^{-1} \text{ Pa}^{-1}] \quad (100)$$

$$K_1(T = 40^\circ\text{C}) = 1.7 \times 10^7 \quad [\text{mol}^{-1} \text{ L}] \quad (101)$$

$$K_2(T = 40^\circ\text{C}) = 2.1 \times 10^3 \quad [\text{mol}^{-1} \text{ L}] \quad (102)$$

$$K_W(T = 40^\circ\text{C}) = 2.9 \times 10^{-14} \quad [\text{mol}^2 \text{ L}^{-2}] \quad (103)$$

As for K_X and K_Y , the values at $T = 15, 25, 35$ and 45°C are summarized in Wang et al. (2011)³¹. Interpolation of these values gives those at $T = 20^\circ\text{C}$ or $T = 40^\circ\text{C}$ as:

$$K_X(T = 20^\circ\text{C}) = 6.9 \times 10^0 \quad [\text{mol}^{-1} \text{ L}] \quad (104)$$

$$K_Y(T = 20^\circ\text{C}) = 2.6 \times 10^7 \quad [\text{mol}^{-1} \text{ L}] \quad (105)$$

$$K_X(T = 40^\circ\text{C}) = 4.7 \times 10^0 \quad [\text{mol}^{-1} \text{ L}] \quad (106)$$

$$K_Y(T = 40^\circ\text{C}) = 5.3 \times 10^6 \quad [\text{mol}^{-1} \text{ L}] \quad (107)$$

Values of $K_{H(\text{NH}_3)}$ and K_b can be obtained from Clegg & Brimblecombe (1989)³² as:

$$K_{H(\text{NH}_3)}(T = 20^\circ\text{C}) = 7.6 \times 10^{-4} \quad [\text{mol L}^{-1} \text{ Pa}^{-1}] \quad (108)$$

$$K_b(T = 20^\circ\text{C}) = 1.7 \times 10^{-5} \quad [\text{mol L}^{-1} \text{ Pa}^{-1}] \quad (109)$$

$$K_{H(\text{NH}_3)}(T = 40^\circ\text{C}) = 3.0 \times 10^{-4} \quad [\text{mol L}^{-1} \text{ Pa}^{-1}] \quad (110)$$

$$K_b(T = 40^\circ\text{C}) = 1.9 \times 10^{-5} \quad [\text{mol L}^{-1} \text{ Pa}^{-1}] \quad (111)$$

Fig.(10) compares the model to the experimental data from Pexton and Badger (1938)³³, using these values. The temperature ranges from $T = 20^\circ\text{C}$ to $T = 40^\circ\text{C}$, while the nitrogen density ranges from $[\text{N}] = 0.128 \text{ mol L}^{-1}$ to $[\text{N}] = 2 \text{ mol L}^{-1}$. Pexton and Badger (1938) provides two independent data sets for each temperature and nitrogen density; one is θ against P_{CO_2} (figures in the left column of Fig.(10)) and the other is P_{NH_3} against P_{CO_2} (figures in the right column of Fig.(10)). These two data sets can be used to validate the model independently.

Fig.(10) shows that the overall shape of the model looks qualitatively consistent with the experimental data both at $T = 20^\circ\text{C}$ and $T = 40^\circ\text{C}$; however, there is an obvious discrepancy in the absolute values. We observed that such discrepancy is minimal in $[\text{N}] = 0.128 \text{ mol L}^{-1}$ and grows as $[\text{N}]$ increases. This trend clearly indicates the influence of ionic strength. Therefore, we need to give an appropriate correction to the values of the seven parameters (namely, $K_{H(\text{CO}_2)}$, $K_{H(\text{NH}_3)}$, K_b , K_1 , K_2 , K_X , K_Y) in the model, according to the change in ionic strength. This is reasonable because the values we substituted into equilibrium coefficients and Henry's constants were those in which the influence of ionic strength is not taken into consideration.

Among the seven parameters, $K_{H(\text{CO}_2)}$, $K_{H(\text{NH}_3)}$ and K_X do not include ionic species in the corresponding reactions. In addition, K_1 and K_Y have the ionic species that have the same charge in the both side of the corresponding reaction. Therefore, it is reasonable to assume that only K_b and K_2 are significantly affected by changes in ionic strength. However, aqueous ammonia contains only a tiny amount of carbonate ions (see Fig.(7)) and indeed a quick parameter test confirms that the model is not very sensitive to the changes in K_2 values. Therefore, we identified K_b as the only parameter that needs to be tuned according to ionic strength.

Based on standard models of ionic strength, Eq.(23) needs to be updated in terms of a thermodynamic equilibrium coefficient $K_{b(\text{therm})}$ ⁴⁰:

$$K_{b(\text{therm})} \equiv \frac{a_{\text{NH}_4^+} a_{\text{OH}^-}}{a_{\text{NH}_3}} \quad (112)$$

$$= K_b \gamma_{\text{NH}_4^+} \gamma_{\text{OH}^-} \quad (113)$$

where, a_i and γ_i represent an activity and an activity coefficient of chemical species i , respectively. Note that K_b is the apparent equilibrium coefficient defined in Eq.(25).

Therefore,

$$K_b = K_{b(\text{therm})} \times \gamma_{\pm}^{-2} \quad (114)$$

where,

$$\gamma_{\pm} \equiv \sqrt{\gamma_{\text{NH}_4^+} \gamma_{\text{OH}^-}} \quad (115)$$

Eq.(114) suggests that we need to multiply γ_{\pm}^{-2} to the original value of K_b . By fitting the model to the experimental data, we derived this multiplier for each [N] as $\gamma_{\pm}^{-2} = 1.8, 2.5, 3.1, 4.0, 4.8$ for [N] = 0.128, 0.5, 1, 1.5, 2 [mol L⁻¹], respectively (see Table.(2)). Fig.(11) shows the model in which these multipliers are applied. This plot demonstrates an excellent agreement between the model and the experimental data both at $T = 20^\circ$ and $T = 40^\circ$.

Fig.(13) shows γ_{\pm} values that were calculated from these multipliers against [N]. To make sure these values of γ_{\pm} are consistent with the Debye-Hückel theory⁴⁰, next, we plot γ_{\pm} against ionic strength, I , which is defined as:

$$I = \frac{1}{2} \sum_i z_i^2 C_i \quad (116)$$

where, C_i and z_i represent concentration and electrochemical valence (negative for anions) of each chemical species i , respectively. Although [N] is an indicator of I that monotonously increases as I increases, ionic strength is not only function of [N] but also of P_{CO_2} , as is shown in Fig.(12). For simplification, we assume that I is virtually constant around the area where experimental data were collected (e.g., at $P_{\text{CO}_2} \sim 2000$ Pa), which is indeed a very good approximation especially in case of smaller [N] (see Fig.(12)). Table.(2) summarizes the ionic strength at $P_{\text{CO}_2} \sim 2000$ Pa. We take an average on the I values at different temperature and regard these values as approximately constant values for each nitrogen density, i.e., $I = 0.107, 0.349, 0.628, 0.913$ and 1.19 [mol L⁻¹] for [N] = 0.128, 0.5, 1, 1.5 and 2 [mol L⁻¹], respectively. These values confirm a linear relation between I and [N]. In Fig.(14), the γ_{\pm} values obtained from the fitting are compared to the Debye-Hückel theory⁴⁰. The Debye-Hückel limiting law, which is valid in very dilute solutions corresponding to ionic strength $< 1 \times 10^{-3}$ mol L⁻¹, is expressed as⁴⁰:

$$\log_{10} \gamma_{\pm} = -A |z_+ z_-| \sqrt{I} \quad (117)$$

where, $A = 0.510 \text{ mol}^{-1/2} \text{ L}^{1/2}$ for water at 25°C ⁴⁰. In our case, $z_+ = 1$ and $z_- = -1$. For moderate concentrations corresponding to ionic strength ranging from 1×10^{-3} mol L⁻¹ to 0.1 mol L⁻¹, the following Debye-Hückel equation⁴⁰ applies:

$$\log_{10} \gamma_{\pm} = -A |z_+ z_-| \frac{\sqrt{I}}{1 + \sqrt{I}} \quad (118)$$

Fig.(14) confirms that the γ_{\pm} obtained from the fitting between the model and experimental data shows a very good agreement with the Debye-Hückel equation at $I \lesssim 0.1$ mol L⁻¹. As ionic

strength gets larger than $\gtrsim 0.1$ mol L⁻¹, the deviation from the Debye-Hückel equation increases, as is expected.

Table 2 Summary of the derived values of γ_{\pm}^{-2} (= multiplier to K_b) and I . I is represented by the value at $P_{\text{CO}_2} \sim 2000$ Pa.

[N] [mol L ⁻¹]	T [°C]	γ_{\pm}^{-2} (= multiplier to K_b)	I [mol L ⁻¹]
0.128	20	1.8	0.118
0.128	40	same as above	0.0960
0.5	20	2.5	0.399
0.5	40	same as above	0.298
1	20	3.1	0.723
1	40	same as above	0.534
1.5	20	4.0	1.04
1.5	40	no data points	0.782
2	20	4.8	1.36
2	40	same as above	1.03

5 Discussion

We have demonstrated that the binary CO₂-H₂O isotherm reduced to the single key analytic equation, Eq.(44), regardless of weak-base, strong-base, aqueous alkaline solutions, aqueous amine solutions or amine solids, which is far from trivial. It is especially notable that, even though this equation includes a square root and several high order terms both in the nominator and the denominator, Fig.(1) through Fig.(9) show that the mathematical structure of this model has indeed very simple but characteristic and non-trivial features. For example, Fig.(2) indicates that the function $\sqrt{1 - \frac{4\alpha\gamma}{\beta^2}} - 1$ has a single maximum value and the functional shape is almost symmetric around that point when it is plotted in linear scale for the vertical axis and in log scale for the horizontal axis, which is almost impossible to tell until one draws the plot. As well as further mathematical investigations on this model, it will be also important to compare this model to the experimental isotherm data. The mathematical framework of the model has been validated using the experimental data from aqueous ammonia (a weak-base aqueous solution) in a quantitative way. Note that this model has already been validated for strong-base quaternary ammonium²⁰. These experimental validations and the theoretical framework developed in this paper indicate that this general model most likely applies to solid amines in the same way; however, experimental validation using solid amines will be necessary in order to strengthen this model furthermore.

It should be noted that the parameters one obtains for different combinations of amines are not independent. For example, the ionic strength effects should be the same for different compositions, affecting K_b of different amines in similar ways. The carbonate/bicarbonate chemistry may be affected by water activity, but is not dependent on the choice of the amine. If different amines are present, their ability to form carbamates or accept protons should be the same in each environment. Therefore, this approach greatly reduces the degrees of freedom one needs to consider in the analysis of complex amine solutions or solids. For example, the moisture swing effect visible in strong-base AEMs should still be present in weak-base AEMs even if it is obscured by other interactions of water with the primary or secondary amine.

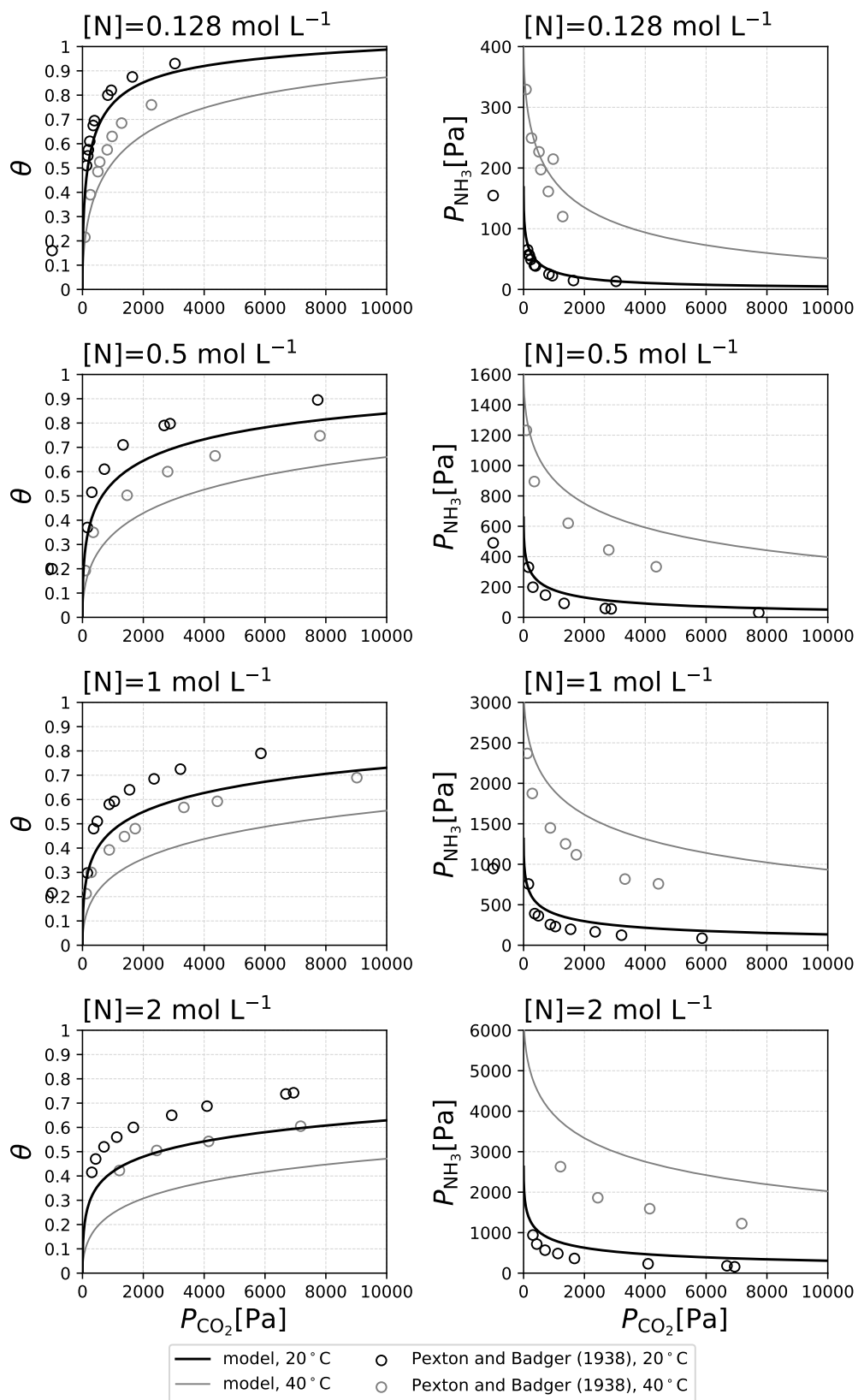


Fig. 10 A comparison of the experimental data from Pexton and Badger (1938) and the model at $T = 20^\circ\text{C}$ or $T = 40^\circ\text{C}$ before influence of ionic strength is corrected. Even though all the data have been used in the fitting procedure, some data points fall outside of the range of the graphs, and are only shown in the Supplementary Information.

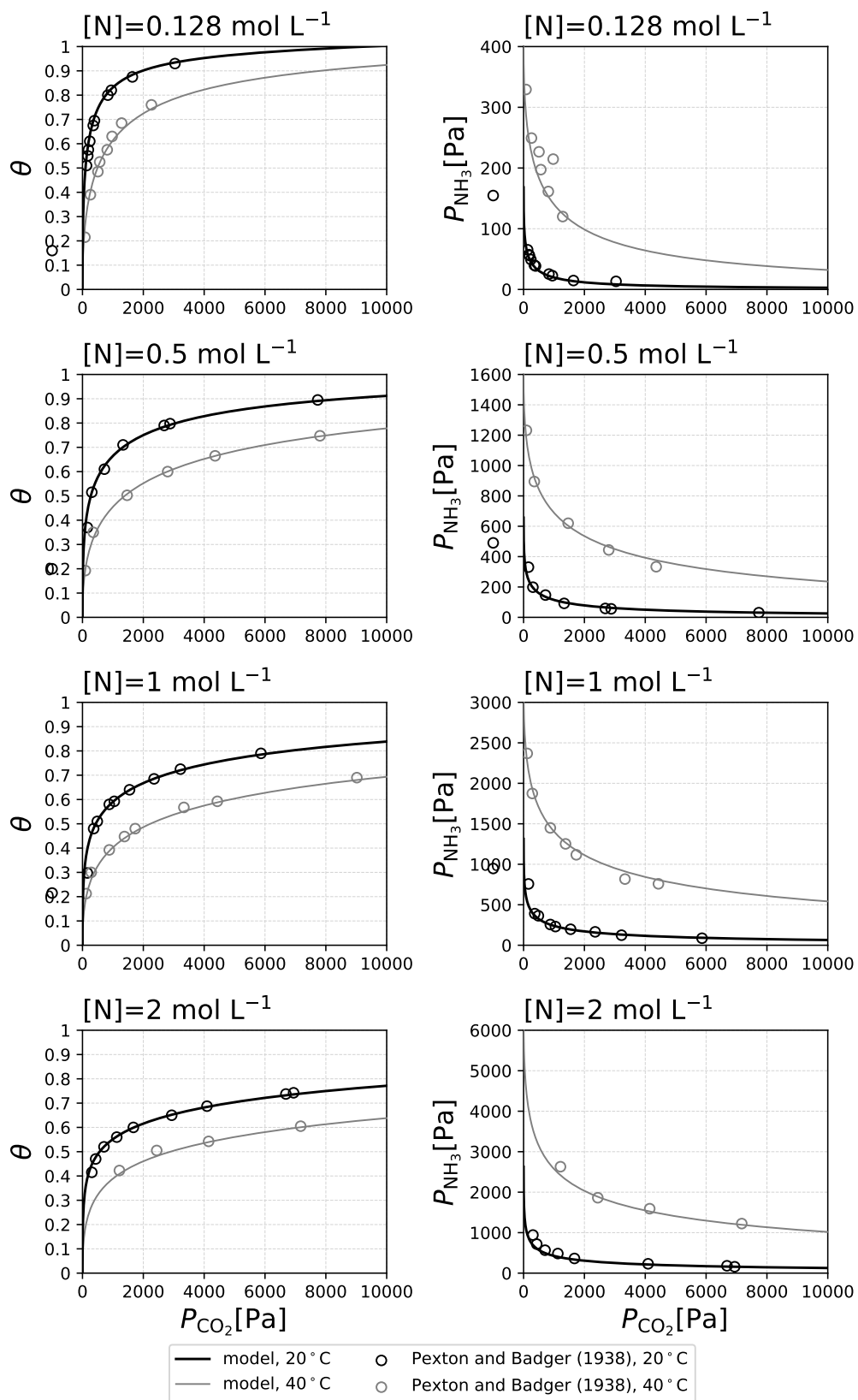


Fig. 11 A comparison of the experimental data from Pexton and Badger (1938) and the model at $T = 20^\circ\text{C}$ or $T = 40^\circ\text{C}$ after γ_{\pm} summarized in Table(2) is applied to correct the influence of ionic strength. Even though all the data have been used in the fitting procedure, some data points fall outside of the range of the graphs. These points are also well fit, and are shown on a logarithmic scale in the Supplementary Information.

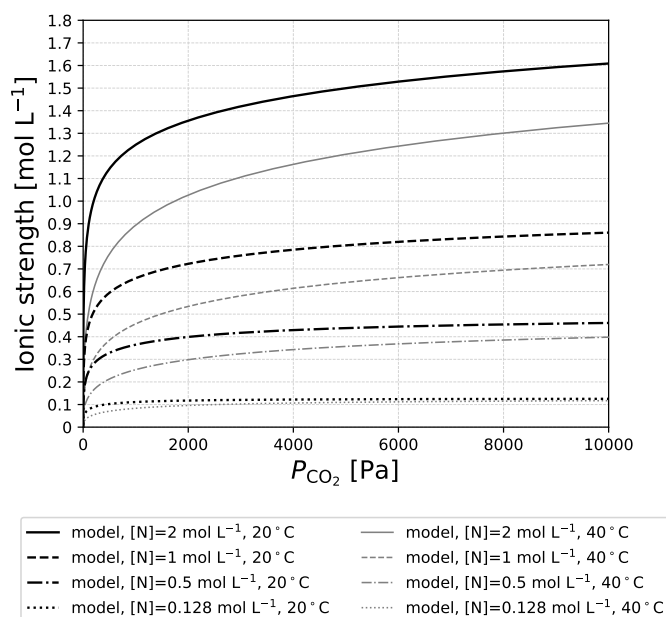


Fig. 12 Ionic strength calculated from the model at $T = 20^\circ\text{C}$ and $T = 40^\circ\text{C}$ and for $[N] = 0.128, 0.5, 1, 1.5$ and 2 $[\text{mol L}^{-1}]$. Note that the γ_{\pm} values have already been applied.

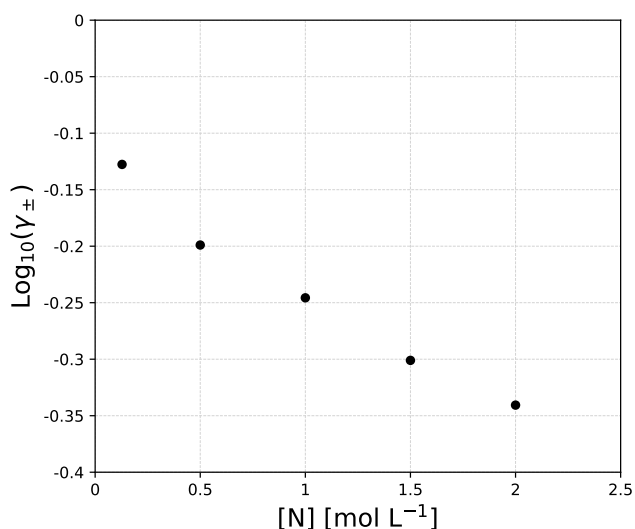


Fig. 13 γ_{\pm} obtained from the fitting between the model and the experimental data in Pexton and Badger (1938) for each $[N]$.

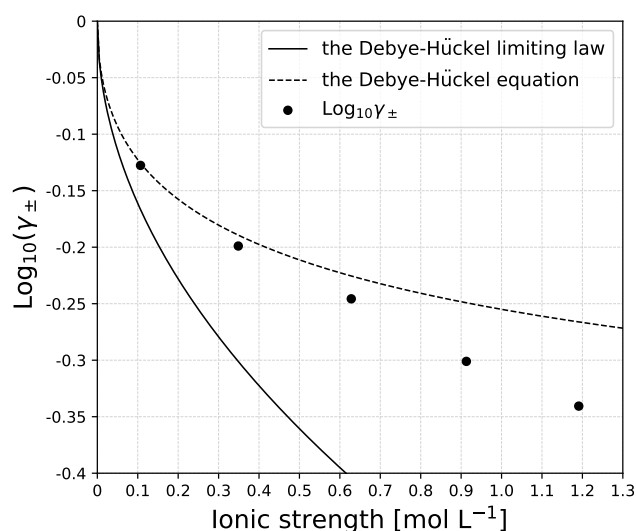


Fig. 14 A comparison between the Debye-Hückel theory and γ_{\pm} values obtained from the fitting.

6 Conclusions

In this paper, first we have identified a single key analytic equation, Eq.(44), which represents a model of CO_2 isotherms and NH_3 isotherms for aqueous ammonia, i.e., a weak-base alkaline solution. It is notable that we can analytically calculate θ or P_{NH_3} from P_{CO_2} and nitrogen density $[N]$ just based on this key equation without relying on complicated numerical solvers. Non-trivial mathematical features of Eq.(44) are explicitly visualized in Fig.(1) through Fig.(9). Also, the asymptotic analysis has been conducted and the results have been summarized in Table.(1), all of which are of theoretical interest.

The predictive capability of this analytic model for weak-base alkaline solutions has been validated using the experimental data of aqueous ammonia at different temperature and nitrogen density in the literature³³, ranging from $T = 20^\circ\text{C}$ to $T = 40^\circ\text{C}$ and from $[N] = 0.128 \text{ mol L}^{-1}$ to $[N] = 2 \text{ mol L}^{-1}$. Initially, we directly compared the model where apparent equilibrium coefficients were used to the experimental data (Fig.(10)). This comparison clarified that influence of the ionic strength needs to be taken into consideration, especially for the solutions of higher $[N]$. Based on theoretical reasoning and a quick parameter test, we identified that K_b is the only relevant parameter which is strongly affected by ionic strength. The activity coefficient γ_{\pm} relevant to K_b has been calculated for $[N] = 0.128, 0.5, 1, 1.5$ and 2 mol L^{-1} by fitting the model to the experimental data (see Table.(2)). Indeed, these γ_{\pm} values yielded an excellent match between the model and the experimental data (Fig.(11)). The calculated values of γ_{\pm} have been compared to the Debye-Hückel theory. As a result, we confirmed that γ_{\pm} shows a very good agreement with the prediction from the Debye-Hückel equation at $I \lesssim 0.1 \text{ mol L}^{-1}$, where the Debye-Hückel equation is supposed to be valid. As ionic strength gets larger than $\gtrsim 0.1 \text{ mol L}^{-1}$, the calculated γ_{\pm} values started deviating from the Debye-Hückel equation, as was expected. Hence, we conclude that this model applies

to aqueous ammonia in a very quantitative way.

This CO₂ isotherm model for weak-base alkaline solution represented by Eq.(44) also applies to strong-base alkaline solutions just by taking a special limit of $K_b \gg [\text{OH}^-]$. In the previous paper, we generalized the CO₂ isotherm theory of strong-base alkaline solutions to that of strong-base anion exchange materials²⁰. In the same way, here we generalized the CO₂ isotherm model for weak-base alkaline solution to amine solutions and finally to solid primary, secondary and tertiary amines in this paper. We can apply essentially the same model for weak-base alkaline solutions (Eq.(44)) to amine solutions but needs to update the values of the three parameters from K_X , K_Y and K_b to K_{XR} , K_{YR} and K_{bR} because it is likely that these values differs from aqueous ammonia to amine solutions. Furthermore, for amine solids, the concentration of water is not large enough to be regarded as constant in the mass action laws unlike in aqueous solutions. Hence, we generalized the model to solid amines by updating K_{YR} , K_{bR} , K_1 and K_2 to $K_{YR(\text{eff})}$, $K_{bR(\text{eff})}$, $K_{1R(\text{eff})}$ and $K_{2R(\text{eff})}$, all of which effectively vary according to the water concentration terms in the corresponding mass action laws. Whether water enhances or hinders CO₂ sorption is determined by stoichiometric coefficients in the elementary chemical reactions when hydration water around the counter ions in the sorbents are taken into consideration.

This work shows that the moisture-swing model that had been established in quaternary ammonium²⁰ was a special case of the general binary CO₂-H₂O isotherm model for amines. The resulting general model is represented by the simple analytic equation, Eq.(44), but can apply to a very wide range of CO₂ sorbents including weak-base or strong-base aqueous alkaline solutions, aqueous amine solutions and solid amines with primary, secondary and tertiary amines. This model allows us to deal with the influence of water in a continuous way so that we will not need to discuss anhydrous states and wet states separately any longer. This analytic model will provide a firm basis for exploring applications of moisture-controlled CO₂ sorption in general amines beyond quaternary ammonium.

Author Contributions

Yuta Kaneko: Conceptualization, Investigation, Methodology, Visualization, Writing (original draft)

Klaus S. Lackner: Conceptualization, Supervision, Validation, Writing (review & editing)

Conflicts of Interest

Klaus S. Lackner is a coinventor of IP owned by Arizona State University (ASU) that relates to certain implementations of direct air capture. Lackner also consults for companies that work on direct air capture. ASU has licensed part of its IP to Carbon Collect and owns a stake in the company. As an employee of the University, Lackner is a technical advisor to the company and in recognition also received shares from the company. Carbon Collect Limited also supports DAC research at ASU.

Acknowledgements

This material is based upon work supported by the U.S. Department of Energy, Office of Science, Office of Basic Energy Sciences

under Award Number DE-SC0023343.

Notes and references

- 1 R. R. Bottoms (Girdler Corp.), *U.S. Patent 1783901, Separating acid gases*, 1930.
- 2 G. T. Rochelle, *Science (American Association for the Advancement of Science)*, 2009, **325**, 1652–1654.
- 3 L. B. Gregory and W. G. Scharmann, *Industrial and engineering chemistry*, 1937, **29**, 514–519.
- 4 F. Goodridge, *Transactions of the Faraday Society*, 1955, **51**, 1703–1709.
- 5 P. Danckwerts, *Chemical engineering science*, 1979, **34**, 443–446.
- 6 T. L. Donaldson and Y. N. Nguyen, *Industrial & engineering chemistry fundamentals*, 1980, **19**, 260–266.
- 7 S. Satyapal, T. Filburn, J. Trela and J. Strange, *Energy & fuels*, 2001, **15**, 250–255.
- 8 K. Foo and B. Hameed, *Chemical engineering journal (Lausanne, Switzerland : 1996)*, 2010, **156**, 2–10.
- 9 C. Gebald, J. A. Wurzbacher, A. Borgschulte, T. Zimmermann and A. Steinfeld, *Environmental science & technology*, 2014, **48**, 2497–2504.
- 10 J. A. Wurzbacher, C. Gebald, S. Brunner and A. Steinfeld, *Chemical engineering journal (Lausanne, Switzerland : 1996)*, 2016, **283**, 1329–.
- 11 S. A. Didas, M. A. Sakwa-Novak, G. S. Foo, C. Sievers and C. W. Jones, *The journal of physical chemistry letters*, 2014, **5**, 4194–4200.
- 12 J. Young, E. Garcia-Diez, S. Garcia and M. van der Spek, *Energy & environmental science*, 2021, **14**, 5377–5394.
- 13 K. S. Lackner, *Thermodynamics of the Humidity Swing Driven Air Capture of Carbon Dioxide*, Grt llc, tucson, az technical report, 2008.
- 14 K. Lackner, *The European physical journal. ST, Special topics*, 2009, **176**, 93–106.
- 15 K. S. Lackner and S. Brennan, *Climatic change*, 2009, **96**, 357–378.
- 16 Y. Kaneko, *Moisture-Controlled CO₂ Sorption and Membranes Actively Pumping CO₂*, 2022.
- 17 T. Wang, K. S. Lackner and A. Wright, *Environmental science & technology*, 2011, **45**, 6670–6675.
- 18 T. Wang, K. S. Lackner and A. B. Wright, *Physical Chemistry Chemical Physics*, 2012, **15**, 504–514.
- 19 X. Shi, H. Xiao, K. Kanamori, A. Yonezu, K. S. Lackner and X. Chen, *Joule*, 2020, **4**, 1823–1837.
- 20 Y. Kaneko and K. S. Lackner, *Physical chemistry chemical physics : PCCP*, 2022, **24**, 14763–14771.
- 21 Y. Kaneko and K. S. Lackner, *Physical chemistry chemical physics : PCCP*, 2022, **24**, 21061–21077.
- 22 T. Suda, M. Iijima, H. Tanaka, S. Mitsuoka and T. Iwaki, *Environmental progress*, 1997, **16**, 200–207.
- 23 P. J. Flory, *Resonance*, 2017, **22**, 416–426.
- 24 R. D. Raharjo, B. D. Freeman and E. S. Sanders, *Journal of membrane science*, 2007, **292**, 45–61.

- 25 G. R. PAZUKI, H. PAHLEVAUZADEH and A. MOHSENI AHOOEI, *Calphad*, 2006, **30**, 27–32.
- 26 H. S. Harned and S. R. Scholes, *Journal of the American Chemical Society*, 1941, **63**, 1706–1709.
- 27 H. S. Harned and R. Davis, *Journal of the American Chemical Society*, 1943, **65**, 2030–2037.
- 28 W. G. Mook, *Environmental isotopes in the hydrological cycle: principles and applications, v. I: Introduction; theory, methods, review*, 2000.
- 29 R. G. Bates and G. D. Pinching, *Journal of the American Chemical Society*, 1950, **72**, 1393–1396.
- 30 F. Christensson, H. C. S. Koefoed, A. C. Petersen and K. Rasmussen, *Acta Chem. Scand. A*, 1978, **32**, 15–17.
- 31 X. Wang, W. Conway, D. Fernandes, G. Lawrance, R. Burns, G. Puxty and M. Maeder, *The journal of physical chemistry. A, Molecules, spectroscopy, kinetics, environment, & general theory*, 2011, **115**, 6405–6412.
- 32 S. L. Clegg and P. Brimblecombe, *Journal of physical chemistry (1952)*, 1989, **93**, 7237–7248.
- 33 S. Pexton and E. Badger, *Journal of Society and Chemical Industry*, 1938, **57**, 107–110.
- 34 V. Darde, K. Thomsen, W. J. van Well, D. Bonalumi, G. Valenti and E. Macchi, *International journal of greenhouse gas control*, 2012, **8**, 61–72.
- 35 V. Darde, B. Maribo-Mogensen, W. J. van Well, E. H. Stenby and K. Thomsen, *International journal of greenhouse gas control*, 2012, **10**, 74–87.
- 36 K. Thomsen and P. Rasmussen, *Chemical engineering science*, 1999, **54**, 1787–1802.
- 37 K. Thomsen, P. Rasmussen and R. Gani, *Chemical engineering science*, 1996, **51**, 3675–3683.
- 38 C.-C. Chen, *Fluid Phase Equilibria*, 1986, **27**, 457–474.
- 39 D. M. Austgen, G. T. Rochelle, X. Peng and C. C. Chen, *Industrial & Engineering Chemistry Research*, 1989, **28**, 1060–1073.
- 40 M. R. Wright, *An introduction to aqueous electrolyte solutions*, John Wiley, Chichester, England ;, 2007.